



# Study of phenolic resin and their tendency for carbon graphitization

Carmen Greice Renda<sup>1</sup> · Roberto Bertholdo<sup>1</sup>

Received: 27 May 2018 / Accepted: 8 October 2018 / Published online: 26 October 2018  
© Springer Nature B.V. 2018

## Abstract

Phenolic resins are important materials in various application sectors due to their outstanding mechanical and thermal properties. However, phenolic resins are known as typical non-graphitized carbon precursor. In this work, important parameters related to the synthesis of PRs were studied: the concentration of the catalyst and the molar ratio between phenol and formaldehyde. The structural information was performed by Fourier Transformation Infrared Spectroscopy and solid state nuclear magnetic resonance of carbon analysis to define mainly between novolac or resol resin. The thermal characteristics of the resins were studied for TGA and their tendencies for graphitization were verified by powder x-ray diffraction and Raman spectroscopy and SEM/HRTEM analysis. As a conclusion, it was verified that the phenolic resins prepared with excess of formaldehyde in acidic medium can present different properties according to their composition, which allows for qualifying them as potential materials for different applications in the technological area that involves graphitized carbon.

**Keywords** Phenolic resin · Carbon precursors · Graphitized carbon · Pyrolytic carbon

## Introduction

Phenolic resins (PRs) based on phenol and formaldehyde are materials widely used in the internal and external parts of automobiles [1], ablative properties [2, 3], aircraft [4, 5], industrial tunnels [6], among others [7–9]. They are important materials in high technology applications, offering reliability, structural integrity, thermal stability and chemical resistance [8, 10, 11]. Among other important applications, PRs have been studied in the construction of floor grids and pipes for offshore oil platforms and refineries [12, 13], in refractories [14, 15], supercapacitors [16] and lithium batteries [17], composites with nanosilica and boron carbide [18], graphene [19], molybdenum [20], lignin and graphene oxide [21, 22]. Phenolic resins' synthesis have received special attention that is why to permit increase their properties [23–25].

Due to its low combustion rate, PRs are widely used in the manufacturing of electrical parts, especially for thermal insulation materials [8, 26], molding compounds, coatings and

composites [5]. When the polymer structure has aromatic rings and absence of paraffin chains, there is a self-retardation of its flammability, without maintenance of the flame, and the product formed releases low levels of smoke and presents a black and graphitic residue [10, 11].

There are polymers able to convert to carbons [27–29]. The potential of thermosetting resins in carbon production, whether in refractories, aerospace or other areas of materials engineering, should be tested in all aspects related to the resin, such as its formulation, processing and pyrolysis of the thermoset [10].

With regard to common carbon precursors, PRs have 80 wt% of their original carbon in their chemical structure, whereas the furan resins have 75 wt% [10]. Carbon precursors can be classified as graphitizable and non-graphitizable, and the phenol/formaldehyde resin is a typical non-graphitized carbon precursor [30].

PRs are produced by the polymerization reaction between phenols and aldehydes or several of their derivatives [5, 15]. The formation of polymer resins based on phenol and formaldehyde comprises three distinct steps: i) Addition of the formaldehyde to the phenol together with the acid or basic catalyst; ii) Growth of the polymer chain or formation of a prepolymer (at temperatures below 100 °C); iii) Occurrence of the curing reaction or crosslinking [5].

✉ Carmen Greice Renda  
carmengreice@gmail.com

<sup>1</sup> Institute of Science and Technology, Federal University of Alfenas, Rodovia José Aurélio Vilela, 11999 – BR 267 Km 533, Poços de Caldas, MG 37715-400, Brazil

With respect to the reaction medium and the molar ratio of phenol and formaldehyde two products could be obtained: a resol resin or a novolac resin. In the strong acidic medium the polymerization reaction starts faster. With lightly alkaline medium the polycondensation reaction is favored, however is necessary the pH correction for stabilized the viscosity [5]. With excess of formaldehyde, with reaction in acidic medium, the obtained resin is novolac and the reaction takes place in two stages. With excess of formaldehyde, with reaction in basic medium, the obtained resin is a resol and the reaction occurs in one step [31].

The mechanisms involved in the reactions of PRs (temperature, stoichiometry, catalysts and pH) have been studied for several specific applications in manufacturing to have their improved characteristics [32–36]. Studies on mechanical analysis of curing, activation energy, molecular weight effects, thermal stability and influence of metals on PRs degradation can be found in the literature [37–41].

In this work, important parameters related to the synthesis of PRs were studied, such as the concentration of the catalyst, the stoichiometric ratio between phenol and formaldehyde, in order to define the structural characteristics of these resins and to verify their tendency for graphitization for future applications.

## Experimental

### Materials

PRs were obtained from the reaction between phenol (99% purity, Proquímios, Brazil) and formaldehyde (36–38 wt% solution, Proquímios Brazil) using hydrochloric acid solution (Vetec, Brazil) as a catalyst.

### Preparation of samples

Phenol and formaldehyde in different molar ratios (see Table 1) were transferred to a beaker in the molar ratios defined in Table 1 and left under magnetic stirring for 30 min. A

**Table 1** Samples varying the concentration of hydrochloric acid,  $[H^+]$ , and molar ratio of phenol and formaldehyde

Samples	$n_{\text{phenol}} / n_{\text{formaldehyde}}$	$[H^+](M)$
PR-1	0.25	12.0
PR-2	0.25	3.20
PR-3	0.25	1.00
PR-4	0.25	0.30
PR-5	0.33	3.20
PR-6	1.00	3.20
PR-7	1.50	3.20
PR-8	2.00	3.20

hydrochloric acid solution at different molar concentrations,  $[H^+]$ , (see Table 1) was added to this mixture (equivalent to 2:3 vol. of HCl:formaldehyde) in order to speed up the reaction rate. The obtained solution was continuously mixed for another 90 min. After that, it was observed that the obtained mixture was comprised by two distinct liquid phases: the first denser and colorless found at the bottom of the beaker (pre-polymer = resin) and; the second a whitish solution at the top (mainly containing un-reacted reagents). The second phase was withdrawn with the use of a pipette and the first one was heated in a 70 °C bath under mechanical stirring for 1–3 min to achieve a major viscosity. The samples were then stored in desiccator for further characterization.

### Characterization

The Fourier Transform Infrared (FTIR) spectra of the samples were obtained with Agilent Technologies Cary 630 FT-IR spectrophotometer in the 4000–650  $\text{cm}^{-1}$  range with 32 accumulations. The diamond ATR accessory proved to be the most convenient to use for both solid and viscous liquid samples synthesized.

The  $^{13}\text{C}$ -CP-MAS-NMR spectra were obtained with a Bruker Avance III HD 400 MHz spectrometer using hexamethylbenzene as internal standard (methyl line at 17.3 ppm), with frequency of 100.568 MHz at room temperature.

The morphological analysis of the bulk PRs dried and covered with the thin carbon film was performed by scanning electron microscopy (SEM) with a Jeol JSM 6510 microscope operating at 2.0 kV.

To investigate the thermal curing properties of PR, Netzsch STA 449 F3 Jupiter Thermal Analysis instrument was used. The mass used for each sample was approximately 10 mg. The covered Platinum crucible was used and the analysis was performed between 30 °C and 1000 °C at a heating rate of 10 °C/min under Argon flux of 50 mL/min.

The carbon samples were prepared in a tubular furnace from phenolic resins under the same conditions related for the TGA analysis. The carbon samples were stored and analyzed by X-Ray diffraction (XRD) and Raman spectroscopy to evaluate the graphitization tendency.

The XRD analysis was obtained with crushed samples with a Rigaku Ultima IV diffractometer using  $\text{Cu K}\alpha$  ( $\lambda = 1,5406 \text{ \AA}$ ) radiation. The diffractograms were collected in  $2\theta$  between 5 and 70° at 1°/min.

A Horiba Scientific Labram HR spectrophotometer coupled to an optical microscope was used to collect the Raman spectra of samples. A He-Ne laser (632.8 nm) with incidence potency of 17  $\mu\text{W}$  over the 200–2000  $\text{cm}^{-1}$  region.

The high resolution transmission electron microscopy (HRTEM) image of the PR-5 sample was performed with a Tecnai G<sup>2</sup> F20 microscope operating at 200 kV. The sample was powered, suspended in ethanol, sonicated during 30 min and collected in a copper grid.

## Results and discussion

### Resin synthesis

Novolac resin is usually expected when reactions happen with excess reagents (phenol or formaldehyde) and acid catalyst [5, 15]. When the acid catalyst is added, the reaction time is faster (total reaction time) and varying the concentration of acid it is possible to control the pre-polymer's viscosity, besides producing a bigger resin amount. In this case, controlled reaction speed was performed in two steps. In the first stage of the forming reaction of phenolic resins, formaldehyde reacts to form crosslinks and intermediary compounds leading to methylene bridges. The acid-catalyzed mechanism involves the protonation of the carbonyl group of formaldehyde followed by electrophilic aromatic substitution of the phenol ring at the ortho-para positions [31].

The similarity among the resol and novolac resins is that both have methylene bridges in linear polymer, and the main difference is that resols have methylol groups ( $-\text{CH}_2\text{OH}$ ) on the ends and in the novolac resins the methylol groups are converted in methylene "bridges" ( $-\text{CH}_2-$ ) with the reaction progress, both linear and between the crosslinked chains, which enables these crosslinking [42].

Figure 1 shows the steps for the methylene bridges formation in the acid catalyzed resins. The structures II and III are typical resol resin, and the structure IV is a possible novolac structure not fully polymerized.

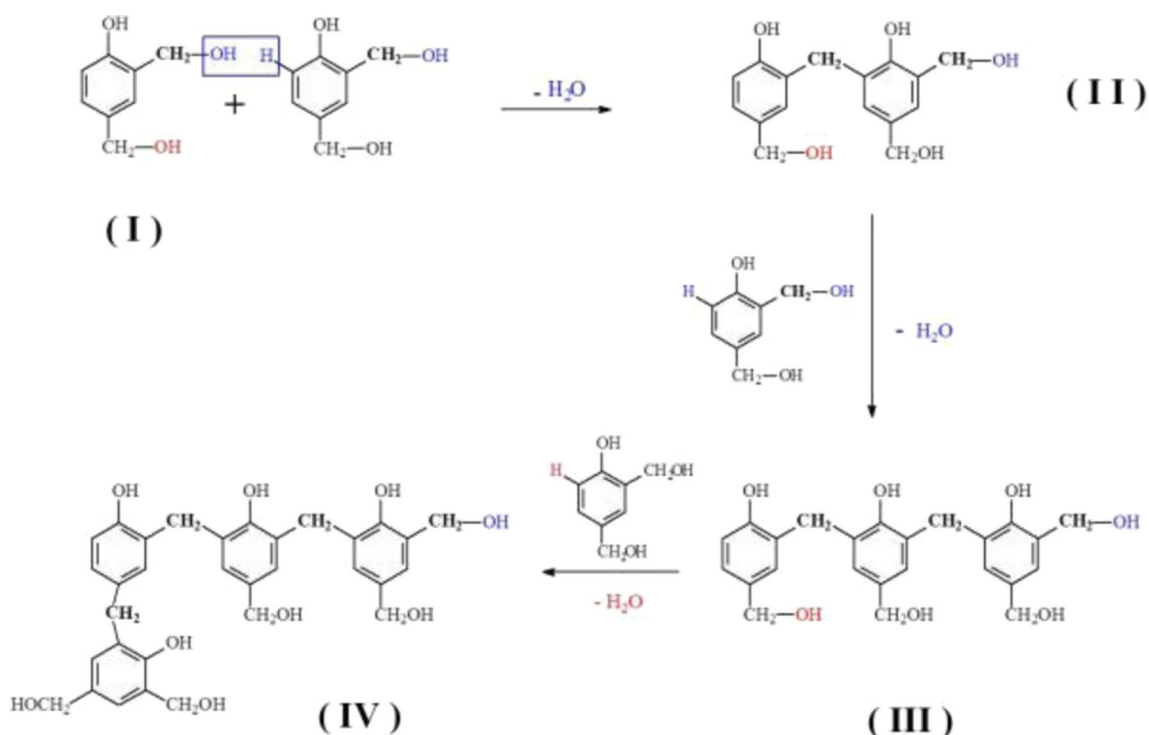


Fig. 1 Steps for the methylene bridges formed in the acid catalyzed resin

### Spectroscopy characterization of the PRs

Figure 2 shows the FTIR spectra of the set of PRs by changing  $[\text{H}^+]$ . Reflectance' intensities are shown in arbitrary units for better visualization, but all the FTIR spectra were normalized, between 0.3 to 1.0, previously. The spectra present a bandwidth around  $3300\text{ cm}^{-1}$  (axial deformation of the intermolecular OH group), bands between  $3010$  and  $2850\text{ cm}^{-1}$  (aliphatic CH axial deformation), bands at  $1601$ ,  $1501$  and  $1475\text{ cm}^{-1}$  (deformation  $\text{C}=\text{C}$  aromatic), bands at  $1454$ ,  $1468$  and  $1444\text{ cm}^{-1}$  (angular strain CH), a band at  $1364\text{ cm}^{-1}$  (angular deformation in the plane of phenol OH), bands at  $1040$ ,  $1023$  and  $1014\text{ cm}^{-1}$  (CO axial deformation in primary alcohols); bands at  $807$  and  $767\text{ cm}^{-1}$  (out-of-plane C-H deformation) [40, 43, 44]. Observing the spectra is the decrease in the band intensity around  $3300\text{ cm}^{-1}$  with the increase of  $[\text{H}^+]$ , indicating the formation of a novolac resin. In addition, the band at  $1475\text{ cm}^{-1}$  shows a higher relative intensity in the PR-1 sample, indicating a greater number of aromatic rings. Thus, the results of these spectra indicate the formation of a polymer with the greatest number of bridges between the aromatic rings as it increases to  $[\text{H}^+]$ . In fact, it was observed that the PR-1 and PR-2 samples were the samples that presented the most rigidity as the main physical characteristic.

Figure 2 shows as greater the concentration of hydrochloric acid  $[\text{H}^+]$  of the final product higher the reflectance's intensities (PR-4 > PR-3 > PR-2 > PR-1).

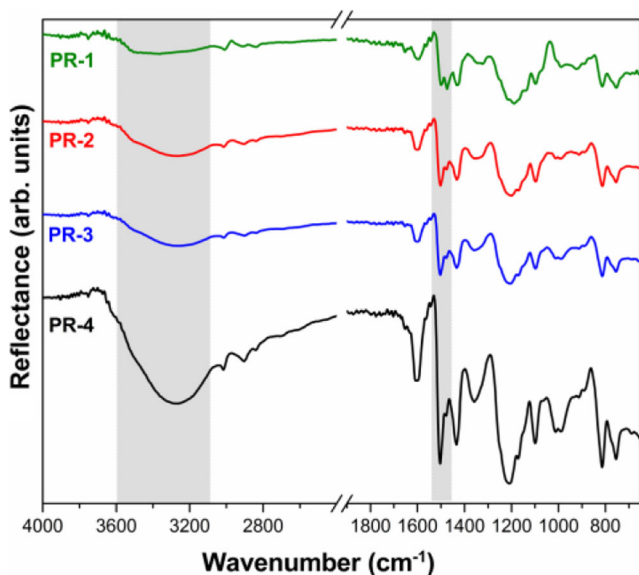


Fig. 2 FTIR spectra of PRs samples with  $[H^+]$  variation

In the Fig. 3, the PRs spectra by varying the molar ratio between phenol and formaldehyde are shown. Analyzing the spectra, it is possible to observe that, with the increase of the amount of formaldehyde in relation to the phenol, the reduction of the bandwidth intensity in  $3300\text{ cm}^{-1}$  and the reduction of the bands in  $1014$  and  $1040\text{ cm}^{-1}$  occurs mainly. The bands at  $1014$  and  $1040\text{ cm}^{-1}$  are assigned to the methylol groups and their decrease indicates the formation of a greater number of crosslinks in this study. In addition, PR-2 and PR-5 samples were found to be solid and rigid, whereas PR-6 to PR-8 samples was in the form of a high viscosity liquid.

Corroborating with this information, normally resol resins present molar weight smaller than novolac ones, with or

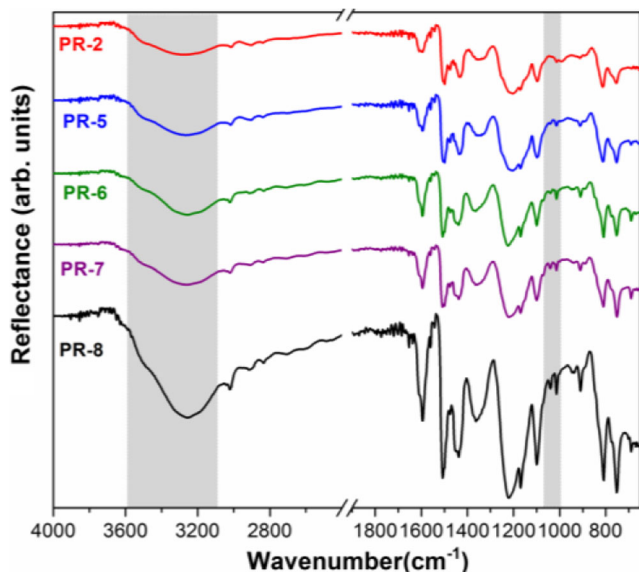


Fig. 3 FTIR spectra of PRs samples with phenol and formaldehyde molar ratio variation

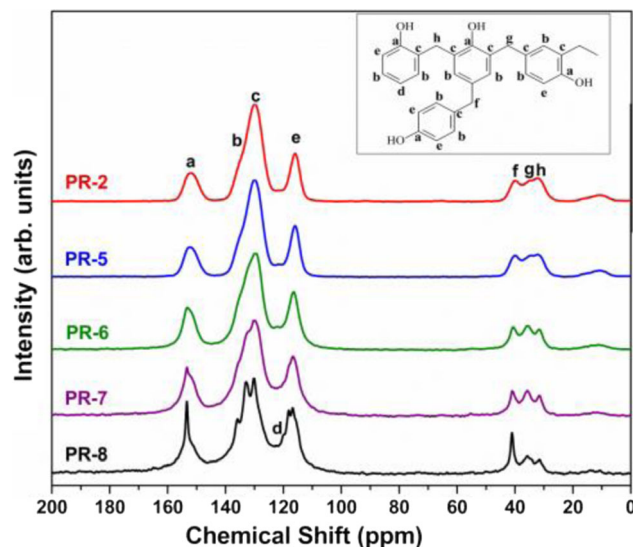


Fig. 4  $^{13}\text{C}$ -CP-MAS-NMR spectra of PRs samples with phenol and formaldehyde molar ratio variation: The positions of identified bands are: a = 151 ppm; b = 135 ppm; c = 130 ppm; d = 120 ppm; e = 116 ppm; f = 40 ppm; g = 35 ppm and; h = 30 ppm

without strong acidic medium as cure agent, and need be store in low temperatures. One advantage of novolac resins is the higher shelf life than resol ones, when stored in room atmosphere [31].

Therefore, these results of FTIR analysis confirm that the reaction with excess formaldehyde in strong acid media lead to the formation of a resin diminished/disappeared the methylol groups (PR-1, PR-2 and PR-5) than are novolac phenolic resins. On the other hand, samples PR-6, PR-7 and PR-8, obtained with the phenol excess in the same acid media, have methylol groups than they were assigned as resol phenolic resins.

Figure 3 shows as greater the solidification of the final product higher the reflectance's intensities (PR-8 > PR-7 or PR-6 > PR-5 > PR-2).

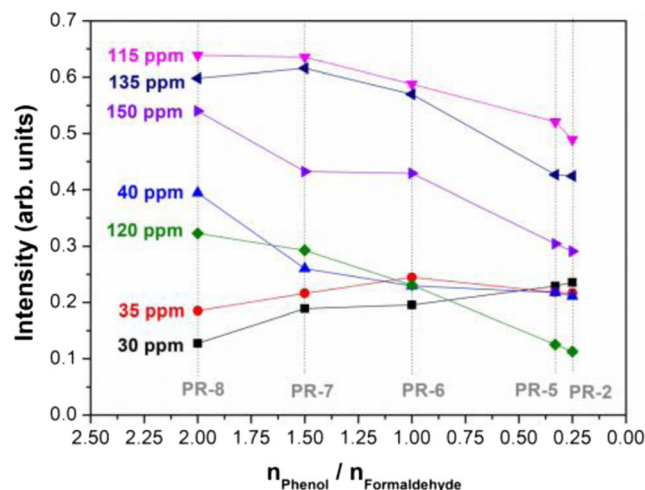
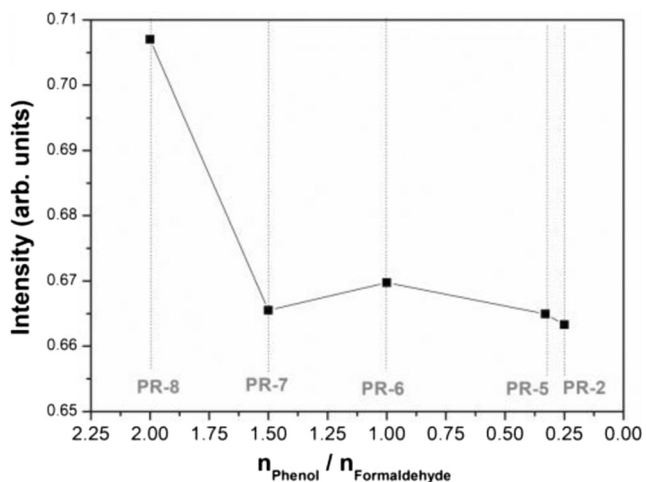


Fig. 5 Trend line of the  $^{13}\text{C}$ -CP-MAS-NMR spectra of PRs samples





**Fig. 6** Trends lines of  $^{13}\text{C}$ -CP-MAS-NMR for the sum of the methylene bridges' intensity varying the phenol/formaldehyde molar ratio

Complementing the structural analysis of the resins, the set of PR with variation of the molar concentration of phenol and formaldehyde was characterized by NMR as shown in Fig. 4.

It is possible to observe that the spectra present very similar bands between samples PR-2 and PR-5, which is not observed in samples PR-6, PR-7 and PR-8. Assignment of the observed bands was performed considering the structure of the polymer shown in the inset of Fig. 4 [45].

Figure 5 shows all the chemical shifts and their intensities, highlight to the increase in 30 ppm and 35 ppm, it can be attributed to ortho-ortho and ortho-para methylene-bridges. It can mean that the material has a predominantly linear

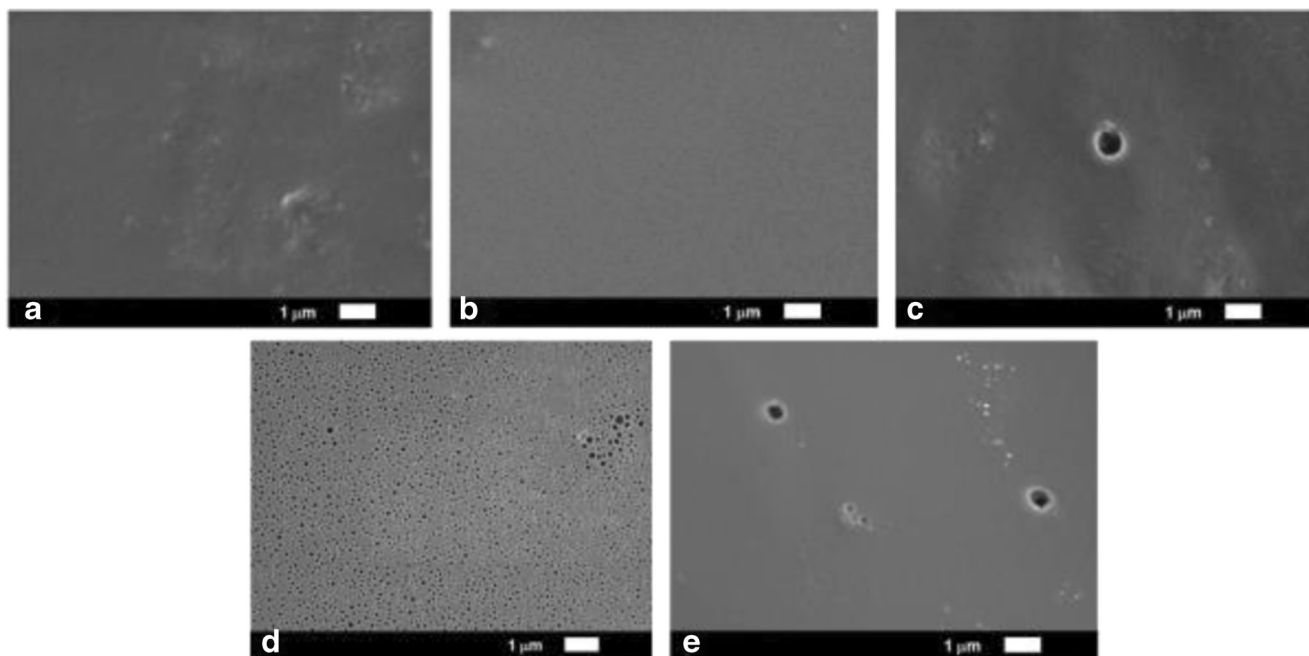
structure, with lightly crosslinking [46], and this behavior can facility the graphitization process. It was founded in the PR-6 and novolac modified resins, PR-2 and PR-5.

Cross-link can improve the thermal stability and char yield of phenolic resins [47] but induces to steric hindrance and lesser mobility to convert in graphitic materials. That is, immobility or miss rearrangement of the carbon atoms during heating means not suffer reconstructive transformation under graphitization conditions [47].

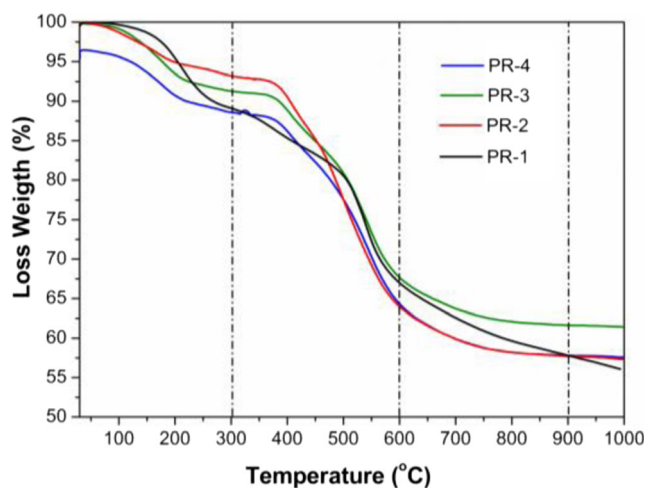
There is necessary the balance between the synthesis/formation of phenolic resins (steric hindrance factors), degradation/pyrolysis mechanisms (volatile compounds) and the carbonization/conversion phase (graphitization).

Figure 6 shows the intensity results obtained from the sum of the methylene bridges' intensity (in the chemical shifts 30 ppm, 35 ppm and 40 ppm, ortho-ortho, ortho-para and para-para methylene bridges respectively).

The overall sum of methylene bridges of novolac resins was lesser than the resol one, but the goal was varying the concentration of acid to control the structure obtained, because this the position of this methylene bridges is so important. In novolac resins the proportion of methylene bridges in ortho-ortho and para-para positions (30 ppm, 35 ppm) is higher than the resol ones, as showed in Fig. 5, probably due the first stage introduced by the variation in the acid, giving mobility to the structure and inducing the carbon'organization. The positions occupied by methylene bridges ( $-\text{CH}_2-$ ) on the first phase of the reaction will be the same as the crosslinking on the second stage' reaction, conferring mobility to the structure for graphitization. PR-8 have not time enough to first stage organization.



**Fig. 7** SEM images of PRs: a PR-8; b PR-7; c PR-6; d PR-5; e PR-2



**Fig. 8** TGA analysis from the set of samples varying  $[H^+]$

PR-2 and PR-5 samples were both obtained with excess formaldehyde in acid medium. Therefore, the amount of excess formaldehyde influences the structure of the novolac resin, which may be related to the kinetic aspects involved in this two step reaction.

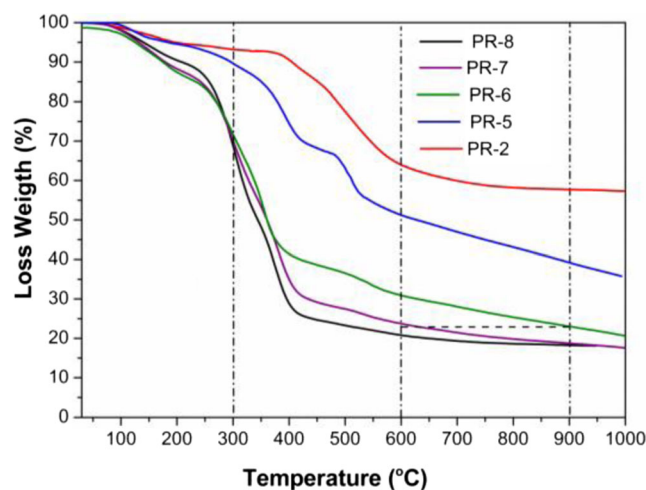
### Morphological characterization of the PRs

Figure 7 shows the SEM images of the phenolic resins obtained by varying the molar ratio of phenol to formaldehyde. In the images, it is possible to note the presence of pores in the novolac samples PR-2, PR-5 and PR-6 and not in the resol resins PR-7 and PR-8. The PR-5 sample was much more porous than the others, with pore diameters between approximately 100 and 300 nm.

Applications can be influenced by the amount of porous on PR-5. For example mesoporous phenolic resin-based carbon can be used for supercapacitors [16] or catalysts systems or scaffolds. The mechanism of pore forming would be the same to the graphitization, due reaction in two stages: the linear product formed in the first stage and more crosslinks in  $-ortho$  and  $-para$  positions on the second stage, and these can improve the chains re-organization in the graphitic planes. The balance between degradation with temperature (minimum

**Table 2** Residual weight at different temperatures for the set of the samples varying  $[H^+]$

Samples	Residual Weight (%)			
	300 °C	600 °C	900 °C	1000 °C
PR-1	89	67	58	56
PR-2	93	64	58	57
PR-3	91	67	62	61
PR-4	89	64	58	58



**Fig. 9** TGA analysis from the set of samples varying molar ratio between phenol and formaldehyde

crosslinking) and steric hindrance (impossible to structure reorganization) is important to the final product obtained.

### Thermal analysis of the PRs

As for the thermal stability of the resins, the information was obtained by TGA. In the set of samples varying  $[H^+]$ , the curves shown in Fig. 8 were obtained.

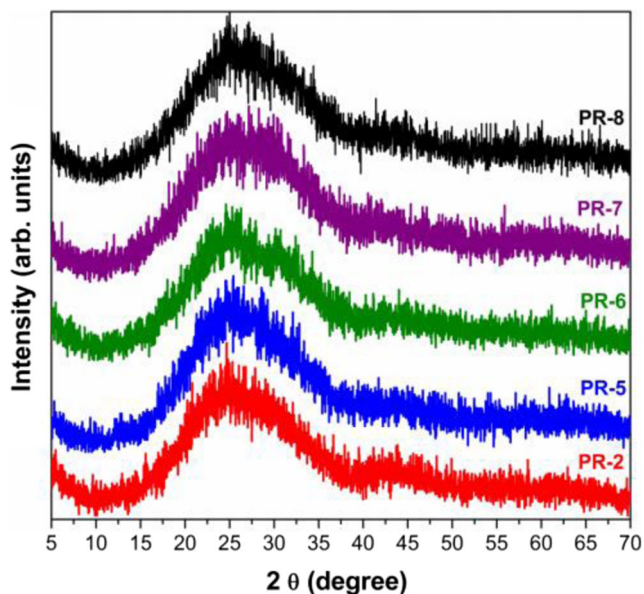
PR-1 should be highest degree of crosslinking according to the synthesis condition thus the higher concentration of hydrochloric acid  $[H^+]$  the reaction time is lower than the others to finish this reaction. The time is another significant factor to obtain highest degree of crosslinking in the  $-ortho$  and  $-para$  positions. It is not possible to have time to complete the first stage and start the second. This reaction had less control from the final product and due this higher degradation with temperature.

Table 2 shows the percentage of residual weight at different temperatures for the set of the samples varying  $[H^+]$ .

The results of Table 2 demonstrate that in the  $[H^+]$  concentration range, the PR-2 sample loses less mass at temperatures below 300 °C. In this temperature range, mass losses are expected by the thermal decomposition of free molecules,

**Table 3** Residual weight at different temperatures for the set of the samples varying the phenol and formaldehyde ratio

Samples	Residual Weight (%)			
	300 °C	600 °C	900 °C	1000 °C
PR-2	93	64	58	57
PR-5	90	51	39	36
PR-6	71	31	23	21
PR-7	70	24	19	18
PR-8	68	21	18	18



**Fig. 10** XRD diffractograms of carbon samples obtained from PRs with molar ratios of phenol and formaldehyde after TGA

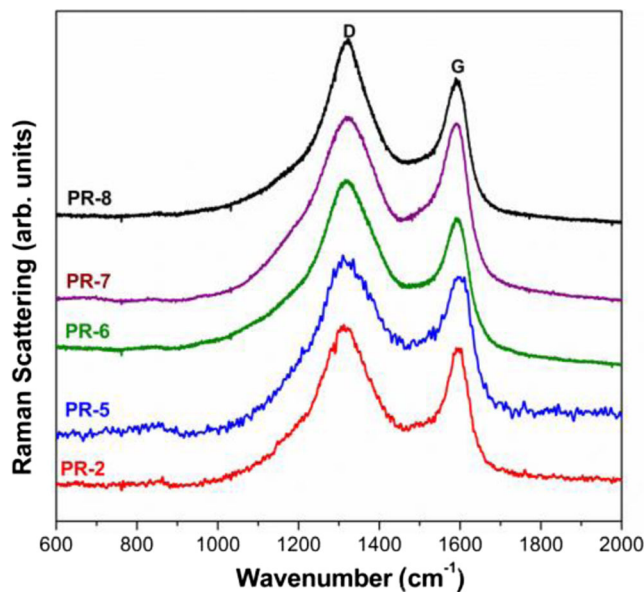


**Fig. 11** Raman spectra of carbon samples obtained from PRs with molar ratios of phenol and formaldehyde after heating treatment up to 1000 °C

reagents excess, catalyst and/or components with imperfect crosslinks or loss of adsorbed water. According to a similar study, this loss consists mainly of water resulting from the reaction of condensation and unreacted monomers [48].

Between 300 and 900 °C, the PR-2 sample accumulates greater mass loss, while the PR-3 sample is the one that least loses mass. In this temperature range, the mass losses may be due to decompositions of the prepolymer components, in where mainly gaseous components such as carbon monoxide, carbon dioxide, methane, phenol, cresols and xylenols are emitted [48].

In the range between 900 and 1000 °C only the PR-1 sample continues to lose mass, while the others are already thermally stable.

The TGA curves of the PRs samples obtained in acid medium with variation of the molar ratio between phenol and formaldehyde are shown in Fig. 9. The results of obtained residual masses are group in Table 3.

In general, it is possible to observe that, in the variation of ratio between phenol and formaldehyde, the samples that lose less mass are the samples PR-2 and PR-5, that is, the samples with excess of formaldehyde or novolac resins. The two

samples with phenol excess PR-7 and PR-8 showed similar thermal behavior between them. As discussed previously, the FTIR results indicated more methylol groups and therefore a resol resin, which justifies this loss of mass observed by TGA, suggesting a higher thermal stability for the novolac resins.

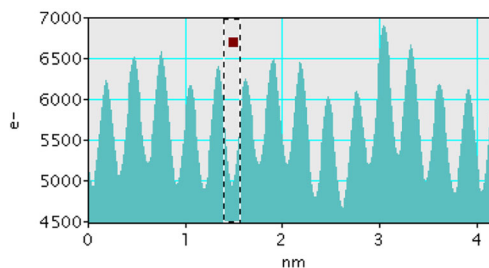
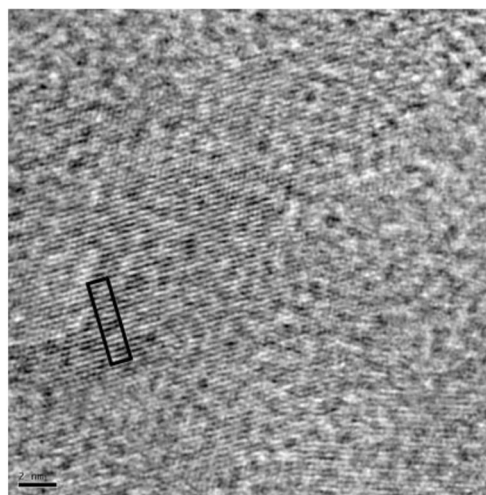


**Fig. 12** HRTEM image to PR-5 sample and profile of frame

**Table 4** XRD and Raman data of the carbons obtained from PRs

Samples	$d_{002}$ (Å)	D position ( $\text{cm}^{-1}$ )	G position ( $\text{cm}^{-1}$ )	$I_D/I_G$
PR-2	3.33	1316	1591	3.15
PR-5	3.34	1325	1590	2.60
PR-6	3.32	1321	1588	4.31
PR-7	3.24	1320	1585	2.99
PR-8	3.26	1320	1587	3.22



## Characterization of carbons samples

Samples of carbons obtained from PRs with molar ratios of phenol and formaldehyde after TGA were analyzed by XRD and Raman spectroscopy.

The XRDs shown in Fig. 10 showed very similar profiles, with a characteristic peak relative to the interplanar distance  $d_{002}$  of the graphite. The enlarged peak indicates the presence of a disordered carbon. The interplanar distances data  $d_{002}$  are summarized in Table 4.

Graphitic planes of graphite are presented in the in the  $2\theta \sim 26^\circ$  (002) e  $\sim 44,2^\circ$  (100) and the non-graphitic planes are presented in  $\sim 24^\circ$  and  $\sim 42^\circ$ . Probably just PR-2 presented a little peak  $\sim 42^\circ$  due the higher graphitization intensity.

The Raman spectra of the samples by varying the molar ratio of the precursors after the TGA analysis are shown in Fig. 11.

Carbon materials have many peaks in the Raman' analyses that can be used to demonstrate the structure organization, many differences are attributed include to the peaks attribution.

Raman spectra showed in Fig. 11 the presence of two major bands: a band around  $1588\text{ cm}^{-1}$ , called the G-band and characteristic for graphitic carbon; A band around  $1320\text{ cm}^{-1}$ , called the D-band and known as disorder band in carbon materials [49]. The results concerning the bands positions and ratios between their intensities ( $I_D/I_G$ ) are shown in Table 4.

Analyzing Table 4, it was found that although the results of XRD indicate the presence of disordered carbon the values of  $d_{002}$  obtained in the PR-5 sample approximate significantly the ideal graphite value ( $d_{002} = 3.354\text{ \AA}$ ) [50]. The  $d_{002}$  value can be used to estimate a graphitization degree of carbon. In addition, the lower value of the  $I_D/I_G$  ratio observed in PR-5 also indicates the presence of a more organized carbon sample than the others. Interlayers different from those obtained by graphitic carbons ( $3.354\text{ \AA}$ ) were cited previously [51, 52].

The results of XRD and Raman suggest that the structure of the polymer obtained directly influences the graphitization process, where the structural differences observed by NMR indicate that the PR-5 sample has a polymer structure with the greatest number of crosslinks that favors graphitization.

Another attributions: D ( $1160\text{ cm}^{-1}$ ), D' ( $1620\text{ cm}^{-1}$ ), D'' ( $1500\text{ cm}^{-1}$ ), I ( $1200\text{ cm}^{-1}$  or  $1330\text{ cm}^{-1}$ ), G' ( $\sim 2700\text{ cm}^{-1}$  with  $G_1'$  and  $G_2'$  – dublets) and  $3200\text{ cm}^{-1}$  [53]. For materials not completely graphitized is better use directly XRD to obtain the structural information's [54]. In this paper, authors prefer simplify and use the first attribution, and use the XRD results and other techniques to complement the characterizations.

Figure 12 shows the PR-5 HRTEM image with graphitizatic carbon closely (2 nm). The amplified area can see the profile of frame with the size average.

Those TEM and HRTEM images corroborating with previous analysis, highlighting organized regions. Phenolic resins with this process of production can be evaluated for thermal, technological and other applications.

## Conclusions

The results concerning the preparation of phenolic resins were presented by varying the amount of catalyst,  $[H^+]$  and the starting materials, phenol and formaldehyde. In these studies, it was found that the larger amount of catalyst increases the number of connected monomeric units, as verified by FTIR. The excess of formaldehyde also converges to the formation of a novolac resin containing crosslinks.  $^{13}\text{C}$ -CP-MAS-NMR spectra confirm the formation of a novolac resin with excess formaldehyde in acid medium and indicate that the PR-5 sample has a number of crosslinks enough to stabilize the structure against the oxidation and it permits some graphitization level as showed in HRTEM.

The TGA results indicated a higher thermal stability of the resins prepared with excess formaldehyde in acidic medium. The carbons obtained after TGA were characterized by XRD and Raman, which showed that the PR-5 resin, which presented the greatest number of crosslinks, gave the formation of a carbon with a higher degree of graphitization.

In conclusion, it was verified that the phenolic resins prepared with excess of formaldehyde in acidic medium can present different properties according to their composition, which allows for qualifying them as potential materials for different applications in the technological area that involves graphitized carbon.

**Acknowledgements** The authors would like to thank Embrapa Instrumentação for SEM and NMR measurements, Laboratório de Cristalografia (UNIFAL-MG) for the XRD measurements, Laboratório de Materiais Fotônicos (LAMF/ UNESP) for the Raman Measurements and Laboratório de Caracterização Estrutural (LCE/UFSCar).

## References

- Hirano K, Asami M (2013) Phenolic resins-100 years of progress and their future. *React Funct Polym* 73:256–269
- Pulci G, Tirillò J, Marra F, Fossati F, Bartuli C, Valente T (2010) Carbon-phenolic ablative materials for re-entry space vehicles: manufacturing and properties. *Compos Part A* 41:1483–1490
- Winya N, Boonpan A, Prapunkarn K (2013) Study of factors affecting the ablation rate of phenolic resin / Fiber glass. *Int J Chem Eng Appl* 4:234–237
- Soutis C (2005) Carbon fiber reinforced plastics in aircraft construction. *Mater Sci Eng A* 412:171–176
- Pilato L (2010) Phenolic resins: a century of progress. Springer-Verlag Berlin Heidelberg, New Jersey
- Binner J, Hogg PJ, Sweeney J (1993) *Advanced materials sourcebook*. Elsevier Advanced Technology, Oxford



7. Lei S, Guo Q, Zhang D, Shi J, Liu L, Wei X (2010) Preparation and properties of the phenolic foams with controllable nanometer pore structure. *J Appl Polym Sci* 117:3345–3550
8. Shen H, Lavoie AJ, Nutt SR (2003) Enhanced peel resistance of fiber reinforced phenolic foams. *Compos Part A* 34:941–948
9. Wang Y, Chen L, Xu T, Yan Y, Gu J, Yun J, Feng J (2017) High char yield novolac modified by Si-B-N-C precursor: thermal stability and structural evolution. *Polym Degrad Stab* 137:184–196
10. Bitencourt CS, Pandolfelli VC (2013) Resinas termofixas e a produção de refratários contendo carbono: base teórica e insights para futuros desenvolvimentos. *Cerâmica* 59:1–26
11. Mano EB (1991) *Polímeros como Materiais de Engenharia*, São Paulo
12. (1999) Suppliers team up for offshore breakthrough. Reinforced plastics. 43(7):16. [https://doi.org/10.1016/S0034-3617\(99\)80058-7](https://doi.org/10.1016/S0034-3617(99)80058-7)
13. (1996) Modified phenolic pipe heats up the offshore market. *Reinf Plast* 40:50–51. [https://doi.org/10.1016/S0034-3617\(98\)80227-0](https://doi.org/10.1016/S0034-3617(98)80227-0)
14. Zhang J, Mei G, Xie Z, Zhao S (2016) Curing mechanism of phenolic resin binder for oxide-carbon refractories. *ISIJ Int* 56:44–49
15. Gardziella A, Pilato LA, Knop A (2000) *Phenolic resins: chemistry, applications, standardization, safety and ecology* 2nd edn. Springer-Verlag, Berlin Heidelberg
16. Chen H, Zhou M, Wang Z, Zhao S, Guan S (2014) Rich nitrogen-doped ordered mesoporous phenolic resin-based carbon for supercapacitors. *Electrochim Acta* 148:187–194
17. Wang M, Fan L (2013) Silicon/carbon nanocomposite pyrolyzed from phenolic resin as anode materials for lithium-ion batteries. *J Power Sources* 244:570–574
18. Haddadi SA, Mahdavian-Ahadi M, Abbasi F (2014) Effect of Nanosilica and boron carbide on adhesion strength of high temperature adhesive based on phenolic resin for graphite bonding. *Ind Eng Chem Res* 53:11747–11754
19. Huang G, Liu H, Yang L, He Y, Xia X, Chen H (2016) Pyrolysis behavior of graphene/phenolic resin composites. *Carbon NY* 98: 733–736
20. Lin C, Lee H, Chen J (2013) Synthesis and characterization of molybdenum/phenolic resin composites binding with aluminum nitride particles for diamond cutters. *Appl Surf Sci* 284:297–307
21. Pérez JM, Oliet M, Alonso MV, Rodríguez F (2009) Cure kinetics of lignin-novolac resins studied by isoconversional methods. *Thermochim Acta* 487:39–42
22. Zhou J, Yao Z, Chen Y, Wei D, Wu Y, Xu T (2013) Mechanical and thermal properties of graphene oxide/phenolic resin composite. *Polym Compos* 34:1245–1249
23. Kapadia M, Patel M, Patel G, Joshi J (2008) La (III) polychelates of phenolic resin: synthesis, characterization and ion-exchange study. *J Polym Res* 15:285–293
24. Patel M, Kapadia M, Joshi J (2009) Polymer-metal complexes of phenolic resin with In (III): thermal, catalytic and antimicrobial aspects. *J Polym Res* 16:755–765
25. Feng J, Chen L, Gu J, He Z, Yun J, Wang X (2016) Synthesis and characterization of aryl boron-containing thermoplastic phenolic resin with high thermal decomposition temperature and char yield. *J Polym Res* 23(97):1–7
26. Desai TG, Lawson JW, Koblinski P (2011) Modeling initial stage of phenolic pyrolysis: graphitic precursor formation and interfacial effects. *Polymer (Guildf)* 52:577–585
27. Chu L, Wang J (2011) Nitrogen removal using biodegradable polymers as carbon source and biofilm carriers in a moving bed biofilm reactor. *Chem Eng J* 170:220–225
28. Takami T, Seino R, Yamazaki K, Ogino T (2014) Graphene film formation on insulating substrates using polymer films as carbon source. *J Phys D Appl Phys* 47:94015
29. Fitzer E, Schaefer W, Yamada S (1969) The formation of glasslike carbon by pyrolysis of polyfurfuryl alcohol and phenolic resin. *Carbon NY* 7:643–648
30. Rand B, McEnaney B (1985) Carbon binders from polymeric resins and pitch, part I - pyrolysis behaviour and structure of the carbons. *Br Ceram Trans J* 84:157–165
31. Borges SG (2004) *Síntese e Caracterização de Resinas Fenólicas Líquidas do Tipo Novolaca Aplicáveis no Processo de Pultrusão Síntese e Caracterização de Resinas Fenólicas Líquidas do Tipo Novolaca Aplicáveis no Processo de Pultrusão*. Universidade Federal do Rio Grande do Sul, UFRGS, Porto Alegre
32. Grenier-Loustalot MF, Larroque S, Grenier P, Leca JP, Bedel D (1994) Phenolic resins: 1. Mechanisms and kinetics of phenol and of the first polycondensates towards formaldehyde in solution. *Polymer (Guildf)* 35:3046–3054
33. Grenier-Loustalot MF, Larroque S, Grande D, Grenier P, Bedel D (1996) Phenolic resins: 2. Influence of catalyst type on reaction mechanisms and kinetics. *Polymer (Guildf)* 37:1363–1369
34. Grenier-Loustalot MF, Larroque S, Grenier P, Bedel D (1996) Phenolic resins: 3. Study of the reactivity of the initial monomers towards formaldehyde at constant pH, temperature and catalyst type. *Polymer (Guildf)* 37:939–953
35. Grenier-Loustalot MF, Larroque S, Grenier P, Bedel D (1996) Phenolic resins: 4. Self-condensation of methylolphenols in formaldehyde-free media. *Polymer (Guildf)* 37:955–964
36. Sojka SA, Wolfe RA, Guenther GD (1981) Formation of phenolic resins: mechanism and time dependence of the reaction of phenol and hexamethylenetetramine as studied by carbon-13 nuclear magnetic resonance and Fourier transform infrared spectroscopy. *Macromolecules* 14:1539–1543
37. Crompton TR (2012) *Thermal stability of polymers*, Smithers Rapra technology ltd, Shawbyry, Shrewsbury, Shropshire. SY4 4NR, UK
38. Lee Y, Kim D, Kim H, Hwang T, Rafailovich M, Sokolov J (2003) Activation energy and curing behavior of Resol- and Novolac-type phenolic resins by differential scanning calorimetry and thermogravimetric analysis. *J Appl Polym Sci* 89:2589–2596
39. Markovic S, Dunjic B, Zlatanic A, Djonlagic J (2001) Dynamic mechanical analysis study of the curing of phenol-formaldehyde novolac resins. *J Appl Polym Sci* 81:1902–1913
40. Carotenuto G, Nicolais L (1999) Kinetic study of phenolic resin cure by IR spectroscopy. *J Appl Polym Sci* 74:2703–2715
41. Wan J, Wang S, Li C, Zhou D, Chen J, Liu Z, Yu L, Fan H, Li BG (2012) Effect of molecular weight and molecular weight distribution on cure reaction of novolac with hexamethylenetetramine and properties of related composites. *Thermochim Acta* 530:32–41
42. Kumar A, Gupta SK, Kumar B, Sumo N (1983) Molecular weight distributions in novolac type phenol-formaldehyde polymerizations. *Polymer (Guildf)* 24:1180–1187
43. Silverstein R, Webster FX, Kiemle DJ (2006) *Identificação Espectrométrica de Compostos Orgânicos* 7.ed edn. Editora LTC, Rio de Janeiro
44. Adabbo HE, Williams RJJ (1982) Curing of Novolacs with para-formaldehyde. *J Appl Polym Sci* 27:893–901
45. Hatfield GR, Maciel GE (1987) Solid-state NMR study of the hexamethylenetetramine curing of phenolic resins. *Macromolecules* 20: 608–615
46. Lenghaus K, Qiao GGH, Solomon DH (2001) 3,5-Dimethylphenol resole resins: their structure and mechanism of thermal decomposition leading to graphitisation. *Polymer (Guildf)* 42:7523–7529
47. Wang Y, Wang S, Bian C, Zhong Y, Jing X (2015) Effect of chemical structure and cross-link density on the heat resistance of phenolic resin. *Polym Degrad Stab* 111:239–246
48. Jones R, Jenkins GM (1976) 9. Volume changes in phenolic resin during carbonization. *Carbon NY* 76:27.6–27.7

49. Ayadi S, Jedidi I, Rivallin M, Gillot F, Lacour S, Cerneaux S, Cretin M, Amar RB (2013) Elaboration and characterization of new conductive porous graphite membranes for electrochemical advanced oxidation processes. *J Membr Sci* 446:42–49
50. Mukhopadhyay P, Gupta RK (2013) 1.4 structural and mechanical characterization of graphite, in: *graph. Graphene their Polym. Nanocomposites*. CRC PRESS - Taylor & Francis Group, Boca Raton, p 21
51. Oya A, Yamashita R, Otani S (1979) Catalytic graphitization of carbons by borons. *Fuel* 58:495–500
52. Liu C, Li K, Li H, Zhang S, Zhang Y (2014) The effect of zirconium incorporation on the thermal stability and carbonized product of phenol-formaldehyde resin. *Polym Degrad Stab* 102:180–185
53. Cuesta A, Dhamelincourt P, Laureyns J, Martínez-Alonso A, Tascón JMD (1994) Raman microprobe studies on carbon materials. *Carbon NY* 32:1523–1532
54. Cuesta A, Dhamelincourt P, Laureyns J, Martínez-Alonso A, Tascón JMD (1998) Comparative performance of X-ray diffraction and Raman microprobe techniques for the study of carbon materials. *J Mater Chem* 8:2875–2879